JOC*Article*

Participation of Multioxidants in the pH Dependence of the Reactivity of Ferrate(VI)

Takashi Kamachi, Tomohisa Kouno, and Kazunari Yoshizawa*

Institute for Materials Chemistry and Engineering, Kyushu University, Fukuoka 812-8581, Japan

kazunari@ms.ifoc.kyushu-u.ac.jp

Received January 17, 2005

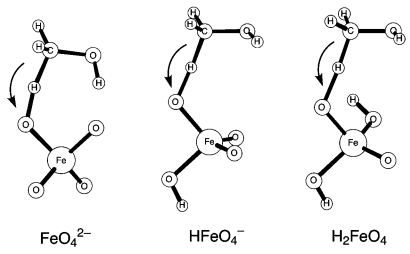

The C–H bond activation by ferrate

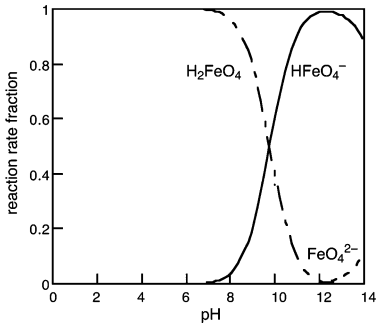

Alcohol oxidation by ferrate (FeO_4^{2-}) in water is investigated from B3LYP density functional theory calculations in the framework of polarizable continuum model. The oxidizing power of three species, nonprotonated, monoprotonated, and diprotonated ferrates, was evaluated. The LUMO energy levels of nonprotonated and monoprotonated ferrates are greatly reduced by solvent effects, and as a result the oxidizing power of these two species is increased enough to effectively mediate a hydrogen-atom abstraction from the C−H and O−H bonds of methanol. The oxidizing power of these oxidants increases in the order nonprotonated ferrate < monoprotonated ferrate < diprotonated ferrate. The reaction pathway is initiated by C−H bond activation, followed by the formation of a hydroxymethyl radical intermediate or an organometallic intermediate with an Fe−C bond. Kinetic aspects of this reaction are analyzed from calculated energy profiles and experimentally known pK_a values. The pH dependence of this reaction in water is explained well in terms of a multioxidant scheme.

1. Introduction

The oxidation of alcohols to aldehydes and ketones is a central reaction in organic synthesis.[1] Traditionally, the transformation has been performed with high-valent transition metal oxides such as manganese dioxide (MnO_2), potassium permanganate ($KMnO_4$), chromium trioxide (CrO_3), potassium chromate (K_2CrO_4), and potassium dichromate ($K_2Cr_2O_7$).[2] However, present stringent ecological standards increase the pressure to develop new, environmentally benign methods. A key to new green oxidation chemistry will be the use and generation of little or no hazardous substances.[3] Ferrate (FeO_4^{2-}) has the potential to become an important green reagent. This is an iron-based oxidant for a variety of organic and inorganic compounds such as alcohols,[4,5] amines,[5,6] hydrazines,[7] peroxides,[8] hydrocarbons,[9] and thiourea[10] with harmless wastes of rust, which is easily separated from desired products.

From an X-ray analysis, ferrate was determined to have a tetrahedral structure as in chromate and manganate.[11] An isotope labeling experiment of oxygen[8] and

* To whom correspondence should be addressed.

(1) *Organic Syntheses by Oxidation with Metal Compounds*; Mijs, W. J., de Jonge, C. R. H. I., Eds.; Plenum: New York, 1986.

(2) (a) *Oxidation in Organic Chemistry*; Wiberg, K. B., Ed.; Academic Press: New York, 1965; Part A. (b) *Oxidation in Organic Chemistry*; Trakanovsky, W. S., Ed.; Academic Press: New York, 1973; Part B. (c) *Comprehensive Organic Synthesis* (*Oxidation*); Trost, B. M., Ed.; Pergamon: New York, 1991; Vol. 7.

(3) Anastas, P. T.; Warner, J. C. *Green Chemistry*: *Theory and Practice*; Oxford University Press: Oxford, UK, 1998.

(4) Audette, R. J.; Quail, J. W.; Smith, P. J. *Tetrahedron Lett.* **1971**, 279.

(5) Tsuda, Y.; Nakajima, S. *Chem. Lett.* **1978**, 1397.

(6) Johnson, M. D.; Hornstein, B. J. *Inorg. Chem.* **2003**, *42*, 6923.

(7) Johnson, M. D.; Hornstein, B. J. *Inorg. Chim. Acta* **1994**, *225*. 145.

(8) Goff, H.; Murmann, R. K. *J. Am. Chem. Soc.* **1971**, *93*, 6058.

(9) Delaude, L.; Laszlo, P. *J. Org. Chem.* **1996**, *61*, 6360.

(10) Sharma, V. K.; Rivera, W.; Joshi, V. N.; Millero, F. J.; O'Connor, D. *Environ. Sci. Technol*. **1999**, *33*, 2645.

10.1021/jo050091o CCC: $30.25 © 2005 American Chemical Society

Published on Web 04/22/2005

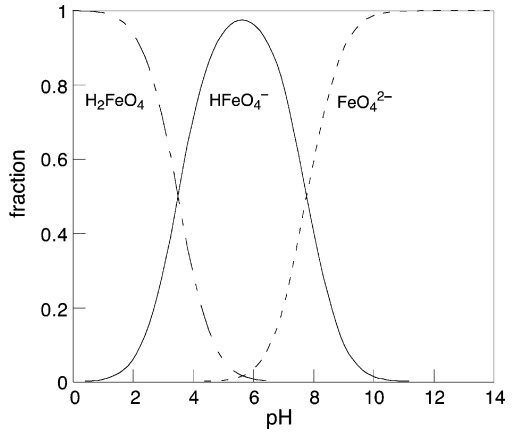

FIGURE 1. Distribution of FeO_4^{2-}, $HFeO_4^-$, and H_2FeO_4 in water as a function of pH.

IR spectroscopy[12] demonstrated that ferrate ion remains monomeric in aqueous solution and that the four oxygen atoms of ferrate are equivalent and exchangeable with solvent water. The stability of ferrate in water is dependent on pH and temperature. It is considerably stable in basic solution above pH 9, while it is reduced by water to evolve O_2 in acidic and neutral solution.[13,14] Reaction rates of alcohol oxidation by ferrate are also known to be highly pH dependent. Norcross et al.[15] measured rate constants for the oxidation of 1,1,1,3,3,3-hexafluoro-2-propanol by ferrate in a pH range from 8.0 to 10.7 and reported that the reaction rate is increased with the acidity of the medium. Their results suggest that the protonation of ferrate ion increases the oxidation power for alcohol oxidation at pH less than 9, as protonated chromate[16] and manganate[17] show stronger oxidation ability.

In a previous paper,[18] we reported the oxidation ability of three ferrate models, nonprotonated ferrate (FeO_4^{2-}), monoprotonated ferrate ($HFeO_4^-$), and diprotonated ferrate (H_2FeO_4), using density functional theory (DFT). Our calculations showed that diprotonated ferrate effectively mediates methanol oxidation via two entrance channels, direct abstraction and addition−elimination processes. On the other hand, B3LYP/6-311G* geometry optimizations did not yield transition states and the methanol-coordinating reactant complex for nonprotonated ferrate and monoprotonated ferrates. These results led us to conclude that FeO_4^{2-} and $HFeO_4^-$ do not have sufficient oxidizing power for methanol in contrast to H_2FeO_4, which is consistent with the experiment mentioned above. However, the distribution of these species as a function of pH,[19] as shown in Figure 1, raises a question about this conclusion. The predominant form is H_2FeO_4 at pH less than 3, $HFeO_4^-$ between 4 and 7, and FeO_4^{2-} above 8. The fraction of the active diprotonated ferrate is lower than 1.2×10^{-5} at a pH range from 8 to 11. Such a trace amount of diprotonated ferrrate is not likely to play an major role in alcohol oxidation by ferrate.

In this study, we reexamine the oxidizing power of ferrate and protonated ferrates in water solvent from DFT calculations in the framework of the polarizable continuum model (PCM). Our new results clearly indicate that inclusion of solvent effects is essential for a proper description of the alcohol oxidation process by ferrate from the viewpoint of structure and energetics. We also investigate the reaction kinetics using information about obtained potential energy diagrams to refine the reaction mechanism. These analyses will increase our understanding of the mechanistic aspects of alcohol oxidation in an aqueous solution of ferrate.

2. Method of Calculation

We used the hybrid B3LYP DFT method[20,21] implemented with the Gaussian 03 program.[22] The B3LYP method has been reported to provide excellent descriptions of various reaction profiles, particularly in geometries, heats of reaction, barrier heights, and molecular vibrations.[23] For the Fe atom the (14s9p5d) primitive set of Wachters' all electron basis set[24] added by one polarization f-function ($\alpha = 1.05$)[25] resulting in a (611111111|51111|311|1) [9s5p3d1f] contraction was used, and for the other atoms the 6-311++G** basis set was used.[26,27] The dielectric effect of water solvent was incorporated by using the polarized continuum model (PCM).[28] All geometries for reaction intermediates and transition states were fully optimized in the aqueous

(11) Hoppe, M. L.; Schlemper, E. O.; Murmann, R. K. *Acta Crystallogr.* **1982**, *B38*, 2237.
(12) Griffith, W. P. *J. Chem. Soc. A* **1966**, 1467.
(13) Wagner, W. F.; Gump, J. R.; Hart, E. N. *Anal. Chem.* **1952**, *24*, 1497.
(14) Wood, R. H. *J. Am. Chem. Soc.* **1958**, *80*, 2038.
(15) Norcross, B. E.; Lewis, W. C.; Gai, H.; Noureldin, N. A.; Lee, D. G. *Can. J. Chem.* **1997**, *75*, 129.
(16) Westheimer, F. H. *Chem. Rev.* **1949**, *45*, 419.
(17) Lee, D. G.; Chen, T. *J. Am. Chem. Soc.* **1993**, *115*, 11231.
(18) Ohta, T.; Kamachi, T.; Shiota, Y.; Yoshizawa, K. *J. Org. Chem.* **2001**, *66*, 4122.
(19) We estimated the distribution of ferrates depending on pH from experimentally known pK_a values.
(20) (a) Becke, A. D. *Phys. Rev. A* **1988**, *38*, 3098. (b) Becke, A. D. *J. Chem. Phys.* **1993**, *98*, 5648.
(21) Lee, C.; Yang, W.; Parr, R. G. *Phys. Rev. B* **1988**, *37*, 785.
(22) Frisch, M. J.; Trucks, G. W.; Schlegel, H. B.; Scuseria, G. E.; Robb, M. A.; Cheeseman, J. R.; Montgomery, J. A., Jr.; Vreven, T.; Kudin, K. N.; Burant, J. C.; Millam, J. M.; Iyengar, S. S.; Tomasi, J.; Barone, V.; Mennucci, B.; Cossi, M.; Scalmani, G.; Rega, N.; Petersson, G. A.; Nakatsuji, H.; Hada, M.; Ehara, M.; Toyota, K.; Fukuda, R.; Hasegawa, J.; Ishida, M.; Nakajima, T.; Honda, Y.; Kitao, O.; Nakai, H.; Klene, M.; Li, X.; Knox, J. E.; Hratchian, H. P.; Cross, J. B.; Adamo, C.; Jaramillo, J.; Gomperts, R.; Stratmann, R. E.; Yazyev, O.; Austin, A. J.; Cammi, R.; Pomelli, C.; Ochterski, J. W.; Ayala, P. Y.; Morokuma, K.; Voth, G. A.; Salvador, P.; Dannenberg, J. J.; Zakrzewski, V. G.; Dapprich, S.; Daniels, A. D.; Strain, M. C.; Farkas, O.; Malick, D. K.; Rabuck, A. D.; Raghavachari, K.; Foresman, J. B.; Ortiz, J. V.; Cui, Q.; Baboul, A. G.; Clifford, S.; Cioslowski, J.; Stefanov, B. B.; Liu, G.; Liashenko, A.; Piskorz, P.; Komaromi, I.; Martin, R. L.; Fox, D. J.; Keith, T.; Al-Laham, M. A.; Peng, C. Y.; Nanayakkara, A.; Challacombe, M.; Gill, P. M. W.; Johnson, B.; Chen, W.; Wong, M. W.; Gonzalez, C.; Pople, J. A. *Gaussian 03*; Gaussian, Inc.: Pittsburgh, PA, 2003.
(23) (a) Baker, J.; Muir, M.; Andzelm, J.; Scheiner, A. In *Chemical Applications of Density-Functional Theory*; Laird, B. B., Ross, R. B., Ziegler, T., Eds.; ACS Symp. Ser. No. 629; American Chemical Society: Washington, DC, 1996. (b) Koch, W.; Holthausen, M. C. *A Chemist's Guide to Density Functional Theory*; Wiley-VCH: Weinheim, Germany, 2000.
(24) Wachters, A. J. H. *J. Chem. Phys.* **1970**, *52*, 1033.
(25) Raghavachari, K.; Trucks, G. W. *J. Chem. Phys.* **1989**, *91*, 1062.
(26) Krishnan, R.; Binkley, J. S.; Seegar, R.; Pople, J. A. *J. Chem. Phys.* **1980**, *72*, 650.
(27) Clark, T.; Chandrasekhar, J.; Spitznagel, G. W.; Schleyer, P. v. R. *J. Comput. Chem.* **1983**, *4*, 294.
(28) (a) Miertus, S.; Scrocco, E.; Tomasi, J. *Chem. Phys.* **1981**, *55*, 117. (b) Miertus, S.; Tomasi, J. *J. Chem. Phys.* **1982**, *65*, 239. (c) Barone, V.; Cossi, M.; Tomasi, J. *J. Chem. Phys.* **1997**, *107*, 3210. (d) Cossi, M.; Barone, V.; Cammi, R.; Tomasi, J. *Chem. Phys. Lett.* **1996**, *225*, 327.

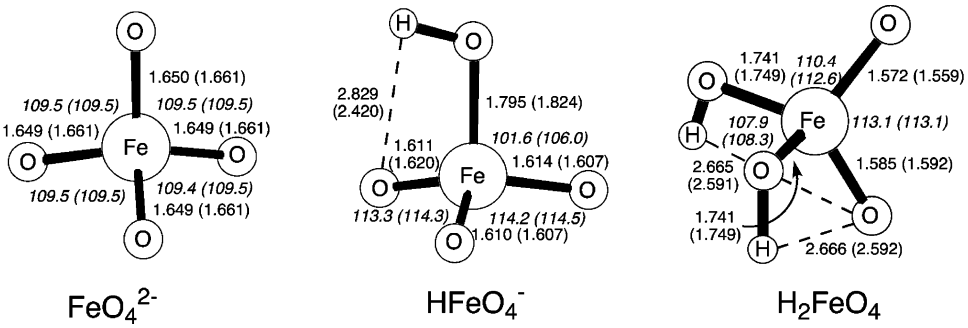

FIGURE 2. Optimized geometries of ferrate and protonated ferrates in the aqueous (gas) phase. Bond distances in Å and angles (italic) in deg.

phase. Vibrational frequencies were systematically computed for all stationary points in order to confirm that each optimized geometry corresponds to a local minimum that has no imaginary frequency or to a saddle point that has only one imaginary frequency. Zero-point energy corrections were taken into account for calculating the energetics of the reaction pathways. The spin state of all species in this study was set to be a triplet according to magnetic susceptibility measurements of the FeO_4^{2-} salts.[29]

3. Results and Discussion

This paper is organized as follows. In section 3.1, geometric and electronic features of the three ferrate models, nonprotonated, monoprotonated, and diprotonated ferrates, in water solvent are discussed. In section 3.2, we look at detailed profiles of computed energy diagrams for methanol oxidation by the three oxidants. Finally, we focus on kinetic aspects of the reaction to reveal the mechanism of the complex pH dependence of the reaction on the basis of computed activation energies for methanol activation. Intermediates and transition states for methanol oxidation by nonprotonated, monoprotonated, and diprotonated ferrates are labeled **n**, **m**, and **d** with numbers, respectively.

3.1. Structures of Ferrate and Protonated Ferrates in Aqueous Solution. Let us first compare geometric and electronic features of ferrate and protonated ferrates in aqueous and gas phases. Figure 2 shows optimized geometries of ferrate and protonated ferrates. Calculated Fe−O distances of 1.65 Å and O−Fe−O bond angles of 109.5° for FeO_4^{2-} in water are in good agreement with an X-ray structure[11] of K_2FeO_4 (Fe−O, 1.65 ± 0.01 Å; O−Fe−O, 109.5°). The $Fe-O_{oxo}$ bonds of ferrate are significantly increased in length upon protonation, while nonprotonated $Fe-O_{oxo}$ bonds are decreased in length. The optimized geometries in aqueous and gas phases are very similar, the maximum deviation for the Fe−O bond distances being 0.029 Å in $HFeO_4^-$.

Table 1 lists computed atomic charges and spin densities of these species. Since Mulliken charges were found to be very sensitive to the choice of basis set in this system,[30] we computed natural population analysis (NPA) charges[31,32] from calculated wave functions of the optimized geometries of these species. The inclusion of solvent effects essentially has no impact on the charge and spin densities of these species. The OH ligands in mono- and diprotonated ferrates have no spin density, and thus the protonation of the oxo ligands of ferrate increases the spin density of the remaining oxo ligands after the reconstruction of the four Fe−O bonds, as seen in the gas phase.[18] Such an increase in the spin density of an oxo ligand promotes a hydrogen atom abstraction from the C−H and O−H bonds of alcohol, this result being consistent with the experimental findings[15] that protonated ferrate has stronger oxidizing ability. In general, solvent effects reduce the LUMO energies of anions. Pearson[33] determined electron affinities in gas and aqueous phases for a large number of anions from gas-phase proton affinities and aqueous pK_a values. All anions exhibit a significant increase of their electron affinity in the aqueous phase, and the solvent effects reduce their LUMO energies compared with those in the gas phase. Safi et al.[34] also observed a decrease in the LUMO energy levels of anions in their ab initio study using the effective fragment potential (EFP) model. The

TABLE 1. Charges (*Q*) and Spin (spin) Densities of Ferrate and Protonated Ferrates in Aqueous and Gas Phases

	FeO_4^{2-}	$HFeO_4^-$	H_2FeO_4
aqueous phase			
Q(Fe)	1.33	1.32	1.36
spin(Fe)	1.35	1.15	1.12
$Q(O_{oxo})^a$	−0.83	−0.65	−0.43
$spin(O_{oxo})^a$	0.16	0.29	0.40
$Q(O_{hydroxo})^a$		−0.38	−0.25
$spin(O_{hydroxo})^a$		−0.02	0.04
gas phase			
Q(Fe)	1.34	1.31	1.35
spin(Fe)	1.32	1.10	1.12
$Q(O_{oxo})^a$	−0.84	−0.62	−0.39
$spin(O_{oxo})^a$	0.17	0.31	0.40
$Q(O_{hydroxo})^a$		−0.45	−0.28
$spin(O_{hydroxo})^a$		−0.03	0.04

[a] Average value.

(29) (a) Hrostowski, H. J.; Scott, A. B. *J. Chem. Phys.* **1950**, *18*, 105. (b) Audette, R. J.; Quail, J. W. *Inorg. Chem.* **1972**, *11*, 1904.
(30) Proft, F. D.; Martin, J. M. L.; Geerlings, P. *Chem. Phys. Lett.* **1996**, *250*, 393.
(31) Reed, A. E.; Curtiss, L. A.; Weinhold, F. *Chem. Rev.* **1988**, *88*, 899.
(32) Weinhold, F.; Carpenter J. E. In *The Structure of Small Molecules and Ions*; Na'aman, R., Vager, Z., Eds.; Plenum Press: New York, 1988.
(33) Pearson, R. G. *J. Am. Chem. Soc.* **1986**, *108*, 6109.
(34) Safi, B.; Balawender, R.; Geerlings, P. *J. Phys. Chem. A* **2001**, *105*, 11102.

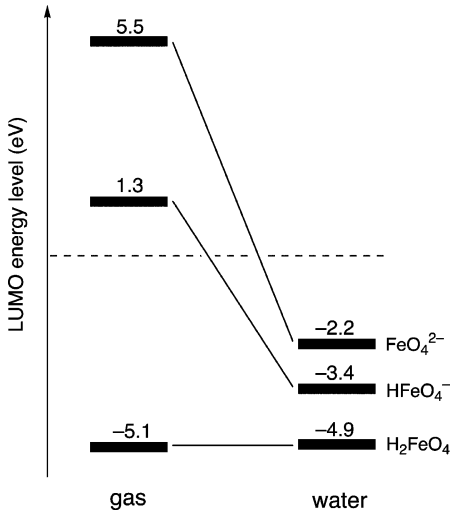

FIGURE 3. The LUMO energy level of ferrate and protonated ferrates in gas and aqueous phases. Solvent effects greatly reduce the LUMO energy of FeO_4^{2-} and $HFeO_4^-$.

LUMO shows a strong energy lowering from 5.5 eV to −2.2 eV in FeO_4^{2-} and from 1.3 eV to −3.4 eV in $HFeO_4^-$, whereas the LUMO of H_2FeO_4 remains almost unchanged in energy, as shown in Figure 3. Thus, the LUMO energy levels of all these species have a minus sign in the aqueous phase. To test the reliability of the B3LYP method in predicting the LUMO energies, we performed single-point calculations at the B3LYP optimized structures of the three oxidants using the B3PW91, BLYP, and BP86 methods. The trends obtained by these methods are consistent as summarized in the Supporting Information. This result clearly shows that the oxidizing abilities of FeO_4^{2-} and $HFeO_4^-$ would be enhanced in the aqueous phase because of the increased electron accepting ability of the two species. In a previous study,[18] we could not locate the transition states and intermediates for a direct hydrogen atom abstraction by FeO_4^{2-} and $HFeO_4^-$ in contrast to H_2FeO_4. The underlying reason for this result may be the high-lying LUMOs of FeO_4^{2-} and $HFeO_4^-$ in the gas phase. We found that FeO_4^{2-} and $HFeO_4^-$ are able to mediate a hydrogen atom abstraction from the C−H and O−H bonds in the aqueous phase, as discussed in the following sections.

3.2. Reaction Pathways for the Conversion of Methanol to Formaldehyde by Ferrates. Let us next look at calculated reaction pathways for the methanol−formaldehyde conversion by nonprotonated and protonated ferrates in the aqueous phase. Previously,[18] we reported two reaction pathways for the alcohol oxidation process by diprotonated ferrate using gas-phase calculations: (1) an addition−elimination mechanism that begins with coordination of methanol to the iron atom and (2) a direct abstraction mechanism that begins with a hydrogen atom abstraction from the O−H or C−H bonds of methanol. We reconsidered these two reaction pathways for alcohol oxidation by nonprotonated and protonated ferrates taking solvent effects into account. An addition−elimination mechanism is initiated by the formation of a methanol-coordinating complex that has an $Fe-O_{methanol}$ bond. We tried in vain to find the methanol-coordinating complex for FeO_4^{2-} and $HFeO_4^-$, while the oxygen atom of a methanol molecule can coordinate to the iron center of diprotonated ferrate with a binding energy of 0.6 kcal/mol, as seen in gas-phase calculations. Optimized geometries of the methanol-coordinating complex for diprotonated ferrate and relevant transitions state for C−H and O−H bond activation are shown in the Supporting Information. Activation energies for the cleavage of the O−H bond of methanol by the oxo and hydroxo ligands of diprotonated ferrate were computed to be 24.2 and 21.8 kcal/mol, respectively. The C−H bond of methanol is also cleaved by the oxo ligand of diprotonated ferrate with an activation barrier of 14.2 kcal/mol. These barriers are rather high compared with a corresponding barrier of 9.2 kcal/mol in the direct abstraction mechanism. For these reasons, we do not discuss the addition−elimination mechanism in detail in this article.

3.2.1. Nonprotonated Ferrate. Figure 4 shows a computed energy diagram and optimized geometries of the reaction intermediates and transition states for the conversion of methanol to formaldehyde by nonprotonated ferrate. Calculated atomic charges and spin densities for these reaction species are listed in the Supporting Information. We named nonprotonated ferrate **1n** for the discussion below. The conversion of methanol is initiated by a direct hydrogen atom abstraction only from a C−H bond of methanol by **1n**. The C−H bond is cleaved by an oxo ligand via **TS(1n→2n)** to yield a radical intermediate (**2n**) in which the hydroxymethyl radical ($^{\bullet}CH_2OH$) is bound to an oxo ligand of ferrate. The activation energy for the hydrogen atom abstraction was computed to be 26.5 kcal/mol relative to the dissociation limit (**1n** + methanol). DFT studies[35,36] on analogous oxidants such as CrO_2Cl_2, MoO_2Cl_2, RuO_4, and MnO_4^- demonstrated that these oxidants should require a higher activation energy for a hydrogen-atom abstraction from a C−H bond. However, this value for nonprotonated ferrate is rather high for a C−H bond activation process by ferrate. We previously investigated the conversion of adamantane mediated by ferrate and protonated ferrates with the B3LYP method in the gas phase.[37] Diprotonated ferrate is found to mediate the activation process of C−H bonds of adamantane with a low barrier of 9.0 kcal/mol from tertiary carbon atoms and of 7.5 kcal/mol from secondary carbon atoms in the triplet spin state. Thus, nonprotonated ferrate is suggested to be a weak oxidant for the C−H bond cleavage as expected from the spin density of the oxo ligand and the energy level of the LUMO. Indeed, nonprotonated ferrate does not have sufficient ability to abstract a hydrogen atom from the more rigid O−H bond of methanol; bond dissociation energies of the C−H and O−H bonds were computed to be 91.8 and 97.6 kcal/mol, respectively, at the B3LYP/6-311++G** level of theory. The transition state involves a nearly linear arrangement with respect to the (Fe)O···H···C moiety. The imaginary frequency mode of the transition state (2031i cm^{-1}) includes the stretching motion of the C−O and O−H bonds. The transition state has an O−H bond of 1.219 Å and a C−H bond of 1.330 Å; these bond distances are typical of the C−H bond activation by various FeO species.

(35) Deng, L.; Ziegler, T. *Organometallics* **1997**, *16*, 716.
(36) Strassner, T.; Houk, K. N. *J. Am. Chem. Soc.* **2000**, *122*, 7821.
(37) Shiota, Y.; Kihara, N.; Kamachi, T.; Yoshizawa, K. *J. Org. Chem.* **2003**, *68*, 3958.

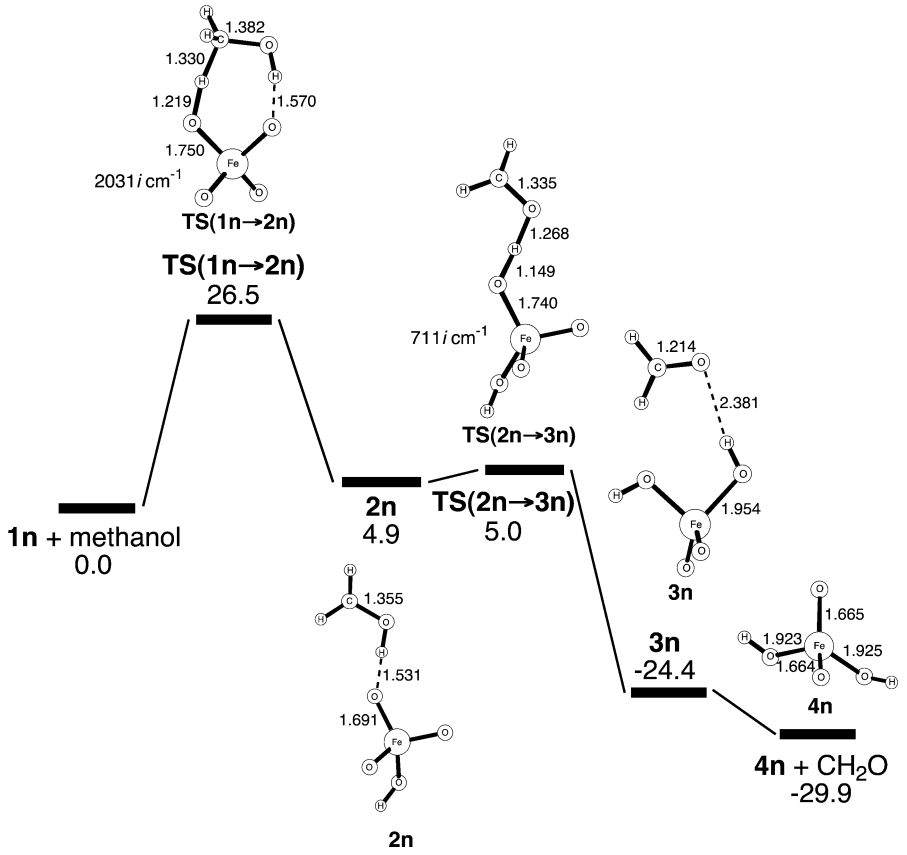

FIGURE 4. Energy profile (in kcal/mol) for the methanol−formaldehyde conversion by ferrate in water. Optimized parameters are shown in Å.

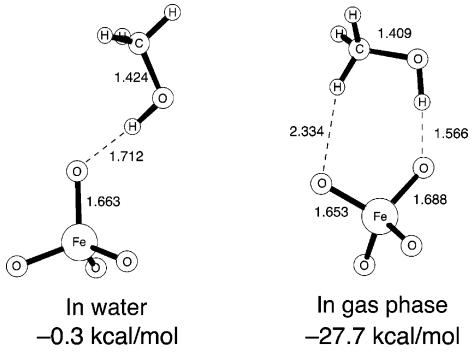

FIGURE 5. Optimized structures of ion−dipole complex in water and gas phases. Units in Å. Relative energies are measured from the dissociation limit.

We looked at an ion−dipole complex of **1n** and a methanol molecule to evaluate the solvent effects on the C−H bond activation process. Figure 5 shows optimized geometries of the complex in water and gas phases. The binding energies between nonprotonated ferrate and methanol were computed to be −0.3 and −22.7 kcal/mol in water and gas phases, respectively, measured from the dissociation limit. These values demonstrate that the methanol molecule is strongly bound to nonprotonated ferrate thorough ion−dipole interactions in the gas phase, while the complex virtually disappears in water due to the strong solvation of the anionic species. A similar phenomenon was reported in theoretical studies on S_N2 reactions between Cl^- and CH_3Cl. Recently, Sato and Sakaki[38] analyzed a typical S_N2 reaction $Cl^- + CH_3Cl \rightarrow ClCH_3 + Cl^-$ using the PCM and RISM-SCF methods. The two methods afforded similar energy profiles for the reaction: solvent effects flatten the ion−dipole potential minimum. On the other hand, the strong ion−dipole interactions can stabilize the reactant complex in the gas phase, binding energy of Cl^- and CH_3Cl being about 10 kcal/mol relative to the dissociation limit. Our results clearly show that a methanol molecule comes into contact with nonprotonated ferrate in the initial stages of this reaction and then a hydrogen atom is abstracted by an oxo ligand in the aqueous phase. In the next step, the O−H bond of the hydroxymethyl radical in **2n** is cleaved via **TS**(**2n**→**3n**) to give rise to an intermediate (**3n**), where the product aldehyde molecule is weakly bound to complex **4n**. The transition state has a small barrier of 0.1 kcal/mol for the O−H bond activation, and thus the O−H bond activation process is substantially barrierless.

3.2.2. Monoprotonated Ferrate. In this section, we consider possible mechanisms of alcohol oxidation by monoprotonated ferrate in water. Figure 6 shows the computed energy diagram and optimized geometries of the reaction intermediates and transition states for the conversion of methanol to formaldehyde by monoprotonated ferrate. As mentioned above, monoprotonated ferrate has an oxidizing ability to activate not only the C−H bond of methanol but also the more rigid O−H bond. In the initial stages of the methanol−formaldehyde conversion, the C−H and O−H activations are compa-

(38) Sato, H.; Sakaki, S. *J. Phys. Chem. A* **2004**, *108*, 1629.

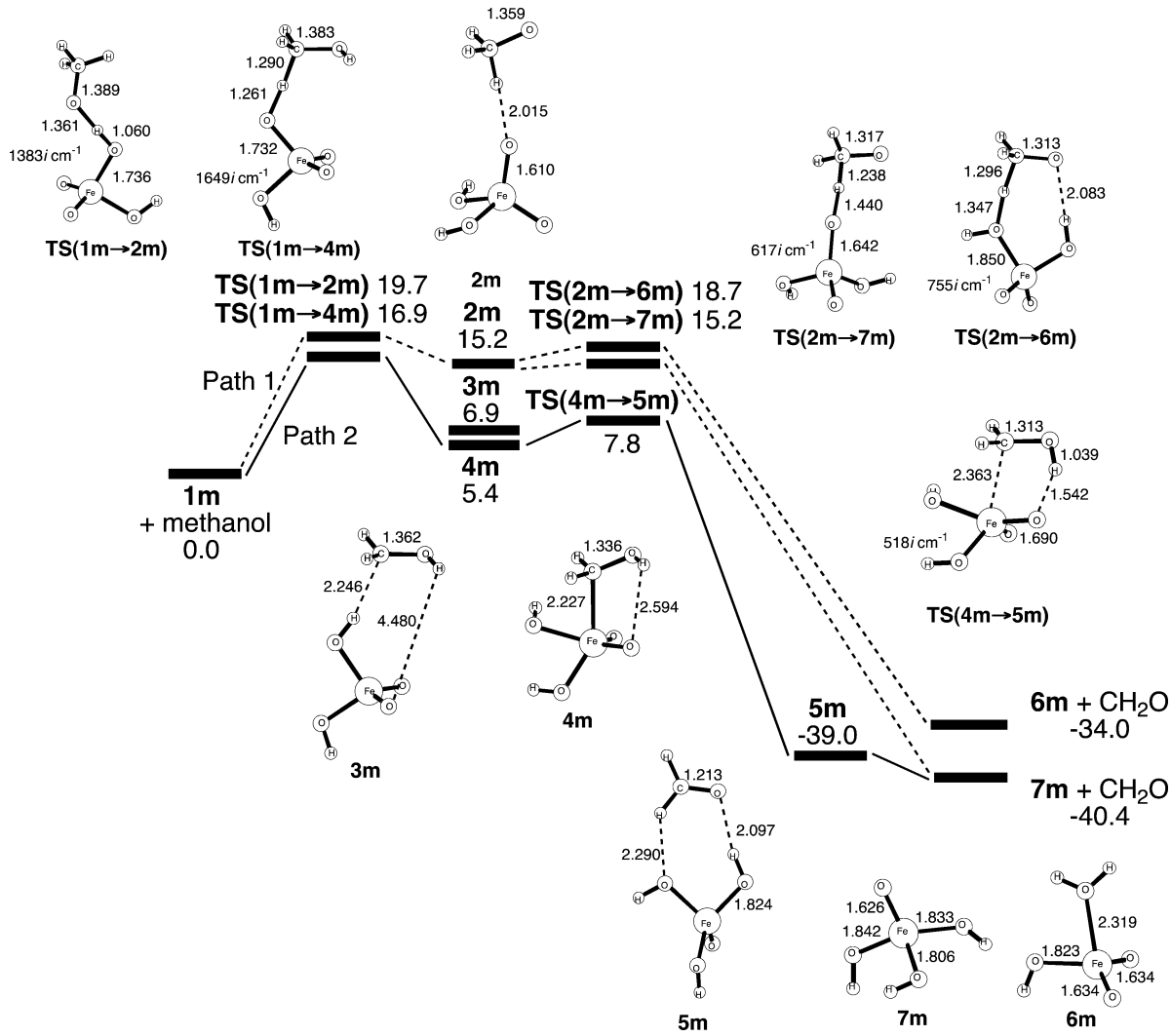

FIGURE 6. Energy profile (in kcal/mol) for the methanol−formaldehyde conversion by monoprotonated ferrate in water. Optimized parameters are shown in Å.

rable in energy.[39] Thus, there are two possible reaction pathways for methanol oxidation by monoprotonated ferrate.

In path 1, the hydrogen atom of the OH group of methanol is first abstracted by an oxo group of monoprotonated ferrate (**1m**) via transition state **TS**(**1m**→**2m**) to form **2m**, in which a methoxy radical is weakly bonded to ferrate. On the other hand, a hydrogen atom abstraction from a C−H bond of methanol occurs in path 2 via **TS**(**1m**→**4m**) to lead to an organometallic intermediate **4m** with an Fe−C bond. We also located a hydroxymethyl radical intermediate **3m**, which lies 1.5 kcal/mol above **4m**. This result indicates that the binding energy between carbon radical center of the hydroxymethyl radical and the iron atom is very small. The activation energies were calculated to be 19.7 kcal/mol for **TS**(**1m**→**2m**) and 16.9 kcal/mol for **TS**(**1m**→**4m**). The activation barrier for the C−H bond activation by monoprotonated ferrate is 9.6 kcal/mol lower than that by nonprotonated ferrate, which supports that protonation of ferrate increases the oxidation power for the C−H bond activation. We also evaluated the oxidizing ability of the hydroxo ligand of monoprotonated ferrate. The transition state for the C−H bond activation by the hydroxo ligand has an O−H bond of 1.371 Å and a C−H bond of 1.241 Å, as shown in the Supporting Information. The calculated barrier for the process is 25.1 kcal/mol, which is 8.2 kcal/mol larger than the value for the oxo ligand.

In the next step of path 1, a C−H bond of the methoxy radical in **2m** is activated either by the oxo or hydroxo ligand to form formaldehyde and complexes **6m** and **7m**. Our calculations show that the C−H bond activation is mainly mediated by the oxo ligand via **TS**(**2m**→**7m**) due to a relatively large energy difference between **TS**(**2m**→**6m**) and **TS**(**2m**→**7m**) of 3.5 kcal/mol. In path 2, the O−H bond of the hydroxymethyl moiety in **4m** is cleaved by an oxo ligand via **TS**(**4m**→**5m**) to form a formaldehyde−ferrate complex **5m**. In view of the calculated energy diagrams the reaction pathway that proceeds through **4m** is the most favorable reaction pathway. This calculational result agrees with the proposal by Lee's group that a key organometallic intermediate with an Fe−C bond is involved in the course of alcohol oxidation by ferrate.[40]

(39) Yoshizawa, K.; Kagawa, Y. *J. Phys. Chem. A* **2000**, *104*, 9347.

(40) Lee, D. G.; Gai, H. *Can. J. Chem.* **1993**, *71*, 1394.

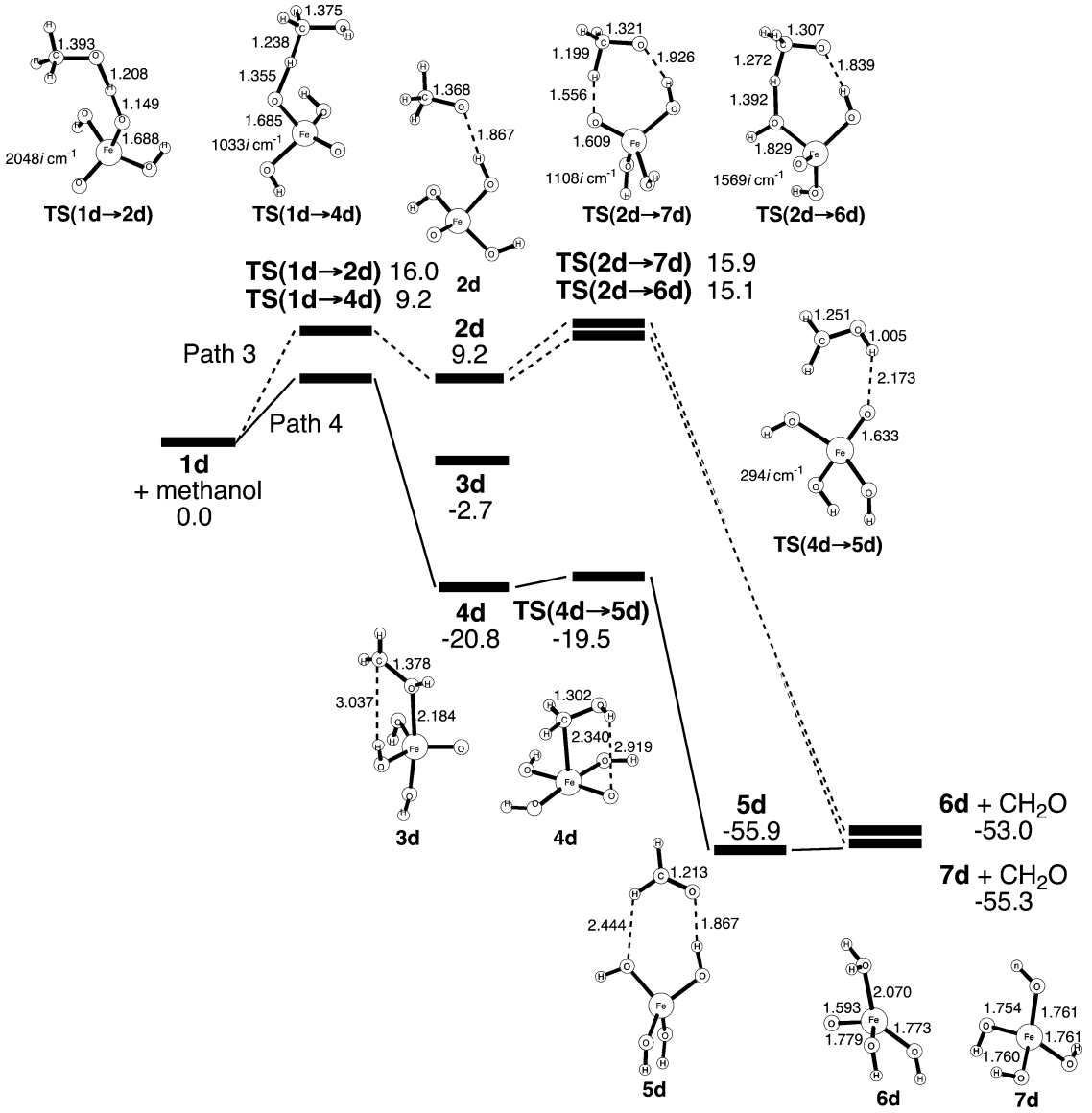

FIGURE 7. Energy profile (in kcal/mol) for the methanol−formaldehyde conversion by diprotonated ferrate in water. Optimized parameters are shown in Å.

3.2.3. Diprotonated Ferrate. In a previous study[18] we considered the energetics for the oxidation of methanol to formaldehyde by diprotonated ferrate in the direct abstraction mechanism. Geometry optimizations of reaction species were performed in the gas phase and after that single-point energy calculations were carried out by the PCM method. Although in the present work we fully optimized the structures of reactant complexes, intermediates, and transition states in water, the calculated potential energy profiles for the process, shown in Figure 7, are essentially identical with the previous ones in the gas phase. Thus, we refer to essential aspects on the reaction pathway here. The activation energies for a hydrogen atom abstraction from the O−H bond (**TS**(**1d**→**2d**)) and a C−H bond (**TS**(**1d**→**4d**)) of methanol are 16.0 and 9.2 kcal/mol, respectively. This result suggests that the C−H bond is preferentially activated by an oxo ligand of diprotonated ferrate. We can reasonably conclude from the calculated activation barriers that diprotonated ferrate has the strongest oxidizing power for methanol oxidation among the three species. A stable organometallic intermediate with an Fe−C bond was found to be produced in this pathway. We cannot find the hydroxymethyl-coordinating intermediate for FeO_4^{2-} and the binding energy between the carbon radical center of the hydroxymethyl radical and the iron atom is very small in **4m** as mentioned above. On the other hand, the corresponding intermediate **4d** in the reaction pathways for diprotonated ferrate has a relatively strong Fe−C bond as indicated by a significant energy over 20 kcal/mol that is released in the course of the Fe−C bond creation. The intermediate is rather stable in energy compared with intermediate **3d** in which the OH group of the hydroxymethyl radical species coordinates to the iron atom. Since the overall reaction is 55.3 kcal/mol exothermic and the transition states involved in this pathway are low lying, the reaction mediated by diprotonated ferrate should easily take place in water.

3.3. Reaction Rate in Water. Our calculational results demonstrate that the order of oxidizing power in

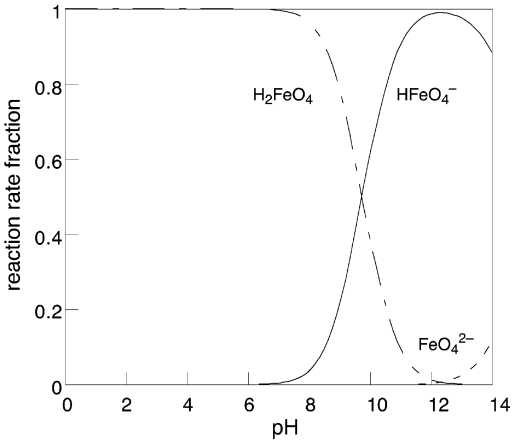

FIGURE 8. Estimated reaction rate fraction of FeO_4^{2-}, $HFeO_4^{2-}$, and H_2FeO_4 in water as a function of pH.

water is diprotonated ferrate > monoprotonated ferrate > nonprotonated ferrate, being in good agreement with a previous result in the gas phase.[18] However, the oxidizing power of the three species is not necessarily a good index to determine which is a main oxidant in alcohol oxidation mediated by ferrate. As discussed above, diprotonated ferrate exists in aqueous solution in extremely small quantities under experimental conditions. Such a trace amount of diprotonated ferrrate is unlikely to be involved as a main oxidant in the reaction. In this section, we consider kinetic aspects of the reaction on the basis of simple kinetics calculations to clarify the relationship between the concentration of these species and the actual reaction rate. The calculated potential energy diagrams show that this oxidation reaction is downhill and highly exothermic and that there is no high barrier after the hydrogen atom abstraction, which is a rate-determining step. Thus, we assumed that the rate law for each pathway is first order with respective to the concentration of oxidant and methanol. The net rate of methanol oxidation is written as follows:

$$-\mathrm{d[M]}/\mathrm{d}t = k_\mathrm{n}[\mathrm{FeO_4}^{2-}][\mathrm{M}] + k_\mathrm{m}[\mathrm{HFeO_4}^{-}][\mathrm{M}] + k_\mathrm{d}[\mathrm{H_2FeO_4}][\mathrm{M}] \quad (1)$$

where [M] is the concentration of methanol and k_n, k_m, and k_d are reaction rate constants for FeO_4^{2-}, $HFeO_4^-$, and H_2FeO_4, respectively. Mono- and diprotonation of FeO_4^{2-} reduce the activation barriers for the hydrogen atom abstraction from a C−H bond by 9.6 and 17.3 kcal/mol, respectively, which leads to the acceleration of reaction rate ($k_\mathrm{m}/k_\mathrm{n} = 1.186 \times 10^7$ and $k_\mathrm{d}/k_\mathrm{n} = 5.149 \times 10^{12}$). We estimated the pH dependence of concentration of these three oxidants from the following equilibria:[41]

$$\mathrm{H_2FeO_4} \rightleftharpoons \mathrm{HFeO_4}^- + \mathrm{H}^+ \qquad \mathrm{p}K_1 = 3.5 \quad (2)$$

$$\mathrm{HFeO_4}^- \rightleftharpoons \mathrm{FeO_4}^{2-} + \mathrm{H}^+ \qquad \mathrm{p}K_2 = 7.8 \quad (3)$$

Figure 8 shows calculated relative reaction rates of FeO_4^{2-}, $HFeO_4^-$, and H_2FeO_4 in water as a function of pH at 25 °C. This illustration clearly demonstrates that the identity of the main oxidant for the reaction is dependent on pH. Interestingly, the main oxidant is $HFeO_4^-$ in strongly basic media, and not H_2FeO_4 that has the strongest oxidizing power among the three oxidants. This result leads us to propose that the concentration of diprotonated ferrate is so low that this powerful oxidant cannot participate in the oxidation reaction. The rate constants of the oxidation of 2-propanol were reported to increase from 0.03 M^{-1} s^{-1} in 3.0 M KOH to 0.14 M^{-1} s^{-1} in 8.0 M KOH.[15] This rate acceleration was proposed to be associated with the formation of a reactive pentacoordinated complex, $HOFeO_4^{3-}$, by the reaction of OH^- ions with FeO_4^{2-}, as proposed in the mechanism of oxidation reactions by RuO_4^- and OsO_4.[42,43] Optimized geometries of $HOFeO_4^{3-}$ and the transition state for the C−H bond activation are shown in the Supporting Information. A calculated activation energy for this transition state is 16.5 kcal/mol relative to the dissociation limit, which indicates that the addition of OH^- to FeO_4^{2-} accelerates the reaction. However, the coordination of OH^- requires 23.7 kcal/mol, and therefore this mechanism is operative only in such an extremely basic solution.

Alcohol oxidation by ferrate is experimentally performed in a pH range of 9−13 to diminish interference from the decomposition of ferrate in aqueous solution as much as possible. Thus, it is difficult to uniquely determine the identity of the active oxidant of the reaction because the hydrogen atom abstraction processes by the two oxidants compete: $FeO_4^{2-}$and $HFeO_4^-$ at pH 12−13 and $HFeO_4^-$ and H_2FeO_4 at pH 9−12, as shown in Figure 8. In fact, numerous kinetic experiments[6,15,44] have suggested the involvement of multiple active oxidants in ferrate reactions. Norcross et al.[15] revealed that the observed pH dependence for the oxidation of 1,1,1,3,3,3-hexafluoro-2-propanol by ferrate was explained well by a kinetic model for the multioxidant process of $FeO_4^{2-}$and $HFeO_4^-$. Thus, our result on the basis of theoretical calculations and experimentally determined pK_a values of ferrate is in good agreement with the complex pH dependence of alcohol oxidation by ferrate in water.

4. Conclusions

We have presented a DFT study of the methanol−formaldehyde conversion by the three active species, FeO_4^{2-}, $HFeO_4^-$, and H_2FeO_4, in water using the polarizable continuum model (PCM). The lowering of the LUMO energy levels of FeO_4^{2-} and $HFeO_4^-$ in water greatly increases the oxidation ability of the two species, while H_2FeO_4 has a strong oxidizing power even in the gas phase because the LUMO energy level of H_2FeO_4 is low in both aqueous and gas phases. We found that the three oxidants effectively mediate the methanol oxidation, in which the C−H and O−H bonds of methanol are homolytically cleaved by the oxo or hydroxo ligands of the oxidants. The most favorable reaction pathway begins

(41) Carr, J. D.; Kelter, P. B.; Tabatabai, A.; Spichal, D.; Erickson, J.; McLaughlin, C. W. Proceedings of the Conference on Water Chlorination and Chemical Environment Impact Health Effects, 1985.

(42) Lee, D. G.; Gai, H. *Can. J. Chem.* **1995**, *73*, 49.

(43) (a) Bales, B. C.; Brown, P.; Dehestani, A.; Mayer, J. M. *J. Am. Chem. Soc.* **2005**, *127*, 2832. (b) Dehestani, A.; Lam, W. H.; Hrovat, D. A.; Davidson, E. R.; Borden, W. T.; Mayer, J. M. *J. Am. Chem. Soc.* **2005**, *127*, 3423.

(44) Johnson, M. D.; Read, J. F. *Inorg. Chem.* **1996**, *35*, 6795.

with the C−H bond activation process, followed by the production of a hydroxymethyl radical intermediate **2n** or an organometallic intermediate **4m** and **4d** with an Fe−C bond. Computed potential energy diagrams show that this oxidation reaction is downhill and highly exothermic and that there is no high barrier after the hydrogen atom abstraction, which indicates that the hydrogen atom abstraction is the rate-determining step in this reaction. The barrier heights of the C−H bond activation by nonprotonated, monoprotonated, and diprotonated ferrates are 26.5, 16.9, and 9.2 kcal/mol, respectively. This result demonstrates that the order of oxidizing power in water is diprotonated ferrate > monoprotonated ferrate > nonprotonated ferrate. To gain a better understanding of the oxidation mechanism in water, we have analyzed the complex pH dependence of this reaction using a simple kinetic model. The calculated relative reaction rate in water indicates that two oxidants compete in this reaction under experimental conditions (pH 9−13), which is in good agreement with the experimentally observed pH dependence of this reaction.

Acknowledgment. K.Y. acknowledges the Ministry of Culture, Sports, Science and Technology of Japan, the Japan Society for the Promotion of Science, Japan Science and Technology Cooperation, and Kyushu University P & P "GreenChemistry" for their support of this work.

Supporting Information Available: Three figures of optimized structures for addition−elimination mechanism, a C−H bond activation by a hydroxo ligand of monoprotonated ferrate, and a C−H bond activation by $HOFeO_4^{3-}$, one table of charge and spin densities of all species, one table of energy levels of the LUMO of ferrate and protonated ferrates for various density functionals, and optimized geometries of all the reaction species. This material is available free of charge via the Internet at http://pubs.acs.org.

JO050091O